

## **Supplementary Information**

### **Gene expression and ultrastructure of meso- and thermophilic methanotrophic consortia**

Viola Krukenberg, Dietmar Riedel, Harald R. Gruber-Vodicka, Pier Luigi Buttigieg,  
Halina E. Tegetmeyer, Antje Boetius, and Gunter Wegener

This file includes supplementary Materials & Methods, Figures and Tables.  
Further supplementary Tables are available as separate excel files.

## Supplementary Materials & Methods

### Origin and cultivation of AOM enrichments

Sediments used in the enrichment of meso- and thermophilic AOM consortia were sampled during the RV Atlantis cruise AT15-56 in November/December 2009 (Alvin Dive 4570) from hydrothermal vent sediments in the Guaymas Basin, Gulf of California, Mexico (27.7438N, 111.409133W; Holler *et al.*, 2011). Material for low-temperature AOM enrichments was collected from shallow water seeps off the coast of Elba, Italy, in 2010 (42.7438N, 10.118233E; Ruff *et al.*, 2016). Enrichments were initiated as described by Holler and colleagues (2011) and Wegener and colleagues (2016). All enrichments were incubated with sulfate reducer medium prepared after Widdel and Bak (1992) and with a headspace composition of CH<sub>4</sub> and CO<sub>2</sub>. We provided methane (0.225 MPa CH<sub>4</sub>(g)), and sulfate (28 mM SO<sub>4</sub><sup>2-</sup> (aq)) as sole electron donor and acceptor, respectively, and carbon dioxide (0.025 MPa CO<sub>2</sub>; 30 mM dissolved inorganic carbon) as carbon source. Parallel enrichments were incubated at 20°C (Elba enrichment; E20), 37°C (Guaymas enrichment; G37) and 60°C (Guaymas enrichment; G60), corresponding to the *in situ* temperature at the sampling site. Culture media were exchanged when sulfide concentrations exceeded ~12 mM and samples were regularly diluted (1:2; 1:4).

### Fluorescence *in situ* hybridization

Aliquots of each AOM enrichment were fixed in 2% formaldehyde for 2 h at room temperature (20-22°C) and washed with 1× phosphate buffered saline (PBS; pH 7.4). Fixed cell suspensions were treated with mild sonication (Sonoplus HD70; Bandelin) and aliquots of 50-250 µl were filtered onto polycarbonate filters (GTTP filters, 0.2 µm pore size, 20 mm diameter). CARD-FISH was performed as previously described (Pernthaler and Amann, 2004) with some modifications, as detailed below. During cell wall permeabilization, filters were sequentially incubated in lysozyme solution (10 mg ml<sup>-1</sup> lysozyme powder, 0.1 M Tris-HCl, 0.05 M EDTA, pH 8) for 15-30 min at 37°C and proteinase K solution (0.45 mU ml<sup>-1</sup> proteinase K (Merck), 0.1 M Tris-HCl, 0.05 M EDTA, pH 8, 0.5 M NaCl) for 2 min at room temperature. To inactivate endogenous peroxidases, filters were incubated in 0.15% H<sub>2</sub>O<sub>2</sub> in methanol (30 min, room temperature). The oligonucleotide probes ANME-1-350, ANME-2-538, HotSeep-1-1456 and SEEP2-658 were applied with formamide concentrations of 40%, 45%, 35% and 45%, respectively (see SI Table 9). To specifically target Seep-SRB2 cells, a competitor (cSEEP2-658; unlabeled version of probe DSS-658) was included with probe Seep-SRB2 to avoid cross hybridization to DSS cells (Kleindienst *et al.*, 2012). For dual

CARD-FISH, peroxidases of the first hybridization were inactivated by incubating the filters in 0.3% H<sub>2</sub>O<sub>2</sub> in methanol (30 min, room temperature). Catalyzed reporter deposition was combined with the fluorochromes Alexa Fluor 488 and Alexa Fluor 594. Filters were stained with DAPI (4,6-diamidino-2-phenylindole). Micrographs were obtained by confocal laser scanning microscopy (LSM 780; Zeiss, Oberkochen, Germany).

### **Extraction of genomic DNA**

Genomic DNA was extracted from ~45 ml of each AOM enrichment (E20, G37, G60). Cells were harvested by centrifugation at 5000 × g for 15 min. The supernatant was discarded and the pellet resuspended in extraction buffer prepared according to Zhou and colleagues (1996). Cell aggregates were disrupted by 40 cycles of manual grinding in a tissue grinder (Wheaton, 1 ml) followed by 3 cycles of freezing in liquid nitrogen and thawing at 65°C. DNA was extracted according to the protocol by Zhou and colleagues (1996) which includes cell lysis by proteinase K digestion, protein denaturation by SDS, nucleic acid purification with chloroform:isoamylalcohol and DNA precipitation with isopropanol at –20°C overnight. Nucleic acids were then collected by centrifugation for 1 h at 13000 rpm and washed three times with ice-cold 70% EtOH (*i.e.* EtOH that has been chilled on ice). The pellet was air dried, re-suspended in PCR grade water and DNA quantity and quality was assessed by measurement with a Qubit instrument (Thermo Fischer) and agarose gel electrophoresis.

For metagenome sequencing, 2-4 µg of high-molecular-weight DNA was used for PCR-free TruSeq paired-end and mate-pair library preparation, following the instructions of the TruSeq library preparation kit. Paired-end libraries were prepared from ~500 bp DNA fragments and mate-pair libraries from DNA fragments of ~5000 bp. Libraries were sequenced on an Illumina MiSeq platform using sequencing chemistry to generate 250 bp reads.

### **Metagenome assembly and draft genome reconstruction**

The quality of raw read data was assessed using FastQC (<http://www.bioinformatics.babraham.ac.uk/projects/fastqc/>). Subsequently, reads were subject to adapter clipping, trimming of their 5' and 3' ends (5 to 10 bases) and removal of reads with quality <20 and length <50 bp using BBDuk (v35.14) (<https://sourceforge.net/projects/bbmap/files/>). Paired-end and mate-pair reads were assembled with SPAdes v3.8.0 (<http://cab.spbu.ru/software/spades/>) using default values of k (21, 33, 55, 77, 99, 127). Binning of the bulk metagenome assembly was performed within the Metawatt software v3.2 (Strous *et al.*, 2012) combining tetranucleotide frequency binning

with manual bin refinement based on coverage and GC spread. Bins of contigs identified as ANME or partner bacterium were extracted from the bulk assembly for targeted reassembly. Paired-end and mate-pair reads were mapped to the binned contigs using BBMap (v. 35.14) (<https://sourceforge.net/projects/bbmap/files/>) with minimum identity of 98% and best site for reads with ambiguous mapping results. Mapped reads and also their unmapped read pairs, were re-assembled using SPAdes (v3.8.0) with default values of k. Assembly quality and bin completeness was assessed using Quast (Gurevich *et al.*, 2013) to obtain general assembly metrics and CheckM (Parks *et al.*, 2015) to provide estimates of the degree of completeness and level of contamination of the bin based on single-copy gene analysis.

### **Extraction of RNA**

Total RNA was extracted from triplicate aliquots (~20 ml) of each enrichment (E20, G37, G60) incubated under the AOM conditions described above. Initially, ~80% culture medium was removed under ambient temperatures and methane headspace. Subsequently, 5 volumes of pre-warmed RNAlater (Sigma-Aldrich, St. Louis, MO) were injected into the remaining biomass to prevent mRNA degradation. Immediately following injection, a 0.15 MPa CH<sub>4</sub>/CO<sub>2</sub> (90/10) headspace was resupplied to the bottles and the RNAlater-amended cultures were kept at ambient temperature for 20 min. Biomass was then collected on polycarbonate filters (GTTP filter, 0.2 µm pore size, 45 mm diameter) via vacuum filtration. Filters were transferred to 2 ml Lysing Matrix E tubes (MP Biomedicals) containing 600 µl of extraction buffer (Quick-RNA MiniPrep kit; Zymo Research, Irvine, CA, USA) for immediate onward processing. Following beat-beating for 2 × 20 sec at power setting 4 in a MP Biomedicals machine, samples were briefly vortexed, centrifuged and their supernatant was collected in a new tube. RNA was extracted from the collected supernatant using the Quick-RNA MiniPrep kit (Zymo Research, Irvine, CA, USA) following manufacturer's recommendations. RNA extracts were treated with DNase I (Roche, Rotkreuz, Switzerland) in the presence of RNasin for 30 min at 37°C followed by DNase I inactivation at 56°C for 10 min. RNA was then purified with the RNeasy MinElute Cleanup kit (Qiagen, Hilden, Germany) following the manufacturer's recommendations and eluted with RNase-free water. RNA quality and quantity was measured on a Bioanalyzer instrument using RNA chips. DNA contamination was tested by a PCR reaction applying previously described primer and cycle conditions for the amplification of archaeal and bacterial 16S rRNA gene fragments (Wegener *et al.*, 2016) but reducing the number of cycles to 15.

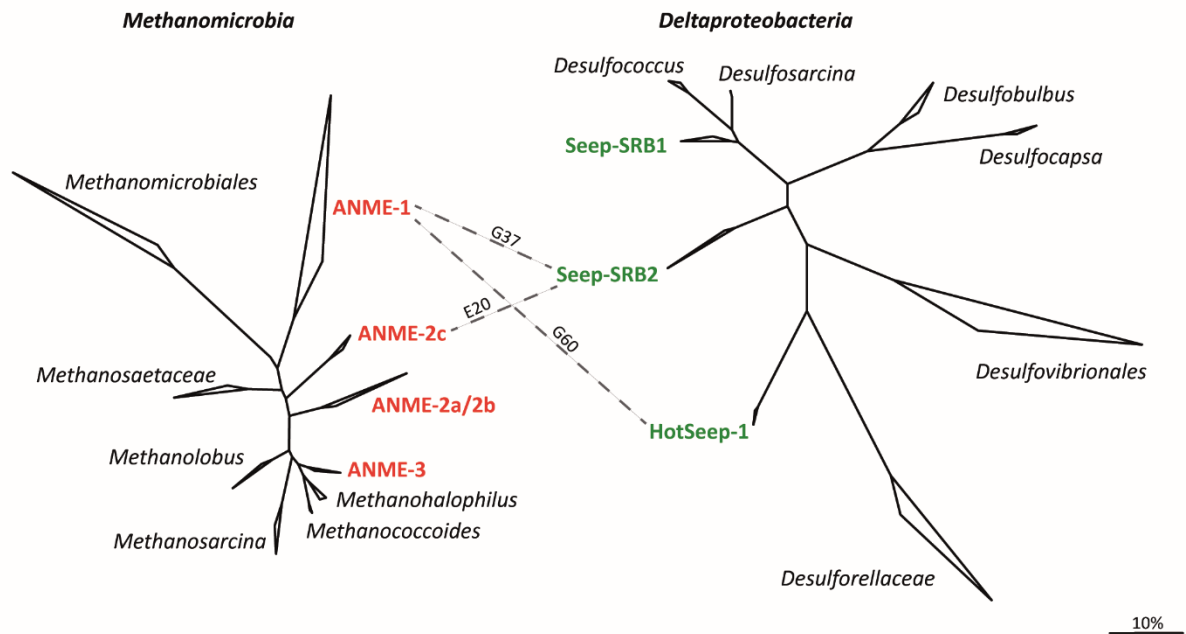
## Heme staining

Heme staining was performed as described by McGlynn and colleagues (2015) with some modifications, detailed below. Aliquots from each enrichment – which included visible precipitates and, in case of G60, visible aggregates – were fixed for 1 h at room temperature with a 0.5 volume of 5% glutaraldehyde (prepared in 25 mM Hepes, pH 7.4, 17.5 g/L NaCl) and a 0.5 volume of 8% paraformaldehyde (prepared in 37.5 mM Hepes, pH 7.4, 26.25 g/L NaCl), resulting in final aldehyde concentrations of 2% paraformaldehyde and 1.25% glutaraldehyde. Fixed samples were washed five times with 1 ml Hepes-buffered saline solution (containing 50 mM Hepes, pH 7.4, 35 g/L NaCl). Each round of washing was performed by centrifugation (1 min, 1000 × g) followed by supernatant removal and resuspension of the pellet in fresh solution. After the final centrifugation step, supernatants were almost completely removed and samples were embedded in 2% agarose (dissolved in 50 mM Hepes, pH 7.4, 35 g/L NaCl) by mixing the sample with the agarose solution in a 0.5 ml PCR tube immediately followed by spinning it down and placing the tube on ice. Once polymerized, the agarose-embedded samples were cut into square blocks. A solution of 3,3'-diaminobenzidine tetrahydrochloride (DAB; Sigma-Aldrich, St. Louis, MO) was prepared by dissolving 0.0543g DAB/ml in 1 M HCl and adding 50 mM Tris-HCl, pH 8 to achieve a final concentration of 0.0015g DAB/ml buffer. The solution was filter-sterilized through a 0.22 µm syringe filter. Heme staining was carried out by incubating the agarose-embedded sample in an aliquot of the DAB solution containing 0.02% H<sub>2</sub>O<sub>2</sub> for 2.5 h. In control experiments, the agarose-embedded sample was incubated in an aliquot of the DAB solution without H<sub>2</sub>O<sub>2</sub>. After incubation, the DAB solution was removed by five 1 ml washes with 100 mM Hepes at pH 7.8. The sample was contrasted by incubation in 0.5 ml of a 1% OsO<sub>4</sub> solution – prepared by dilution of a 4% aqueous stock into 100 mM Hepes, pH 7.8 solution – for 90 min on ice and then washed five times with 1 ml of 100 mM Hepes, pH 8 solution. Finally, samples were dehydrated by washing with increasing concentrations of ethanol (2 washes of 5 min each using 50%, 70%, 100% v/v EtOH and 2 × 10 min 100%) and propylene oxide (1 × 10 min), followed by infiltration with a mixture of Agar100 (Epon 812 equivalent) and propylene oxide (3 incubations of 5 min each, in 1:1, 2:1, 3:1 v/v mixtures of Agar100:propylene oxide) and Agar100 (2 incubations of 5 min, 1 incubation of 1 h and 1 incubation overnight). Following the overnight incubation, samples were transferred to fresh Agar100, placed into embedding moulds and the embedding medium was allowed to polymerize for 3 days at 60°C.

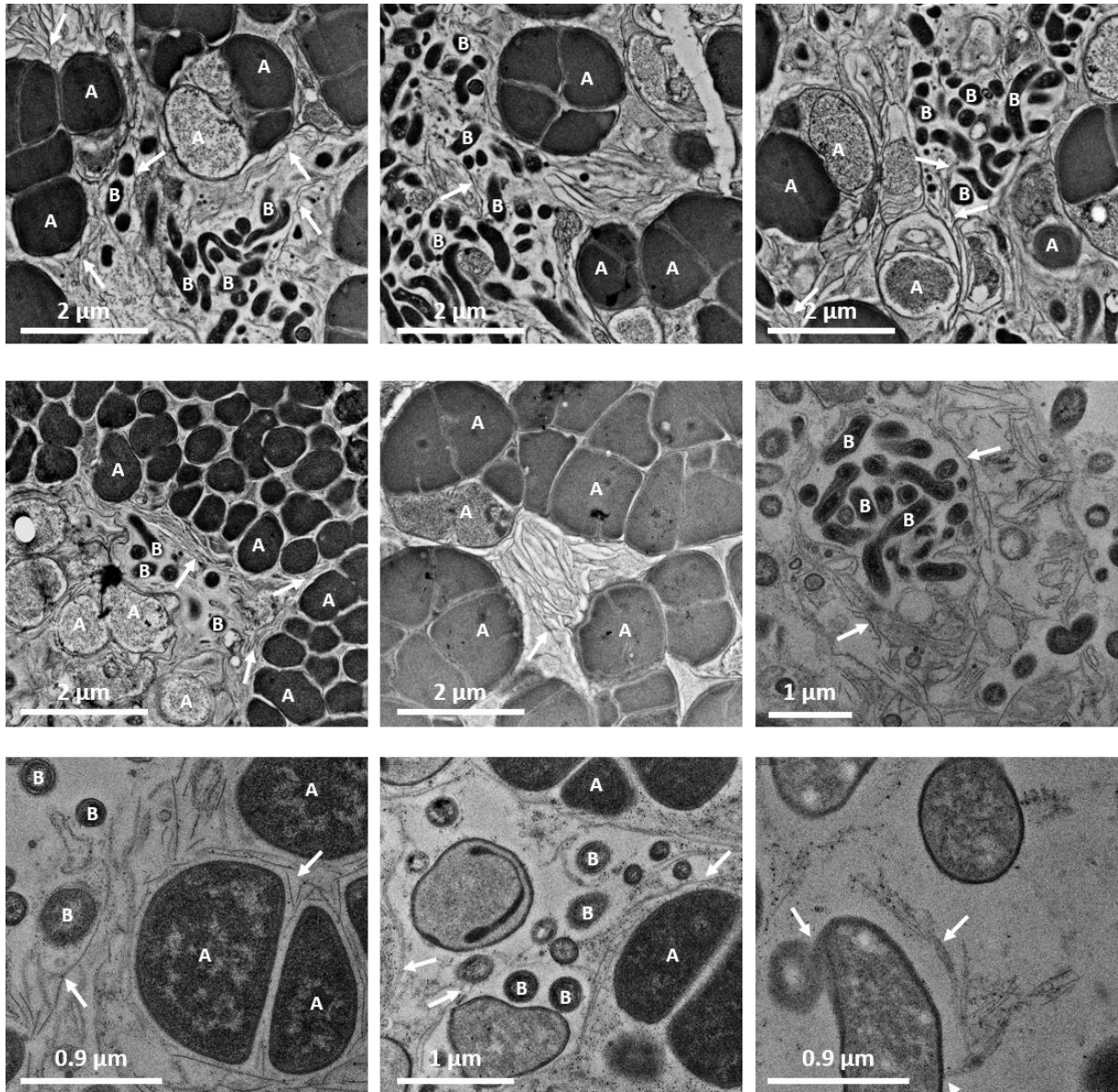
### **Transmission electron microscopy**

As described previously (Wegener *et al.*, 2015) AOM consortia were placed on a flat embedding specimen holder (Leica Microsystems, Wetzlar, D-35578 Germany) and frozen in a Leica EM PACT high pressure freezer. Once the cells have been vitrified they may be stored in liquid nitrogen indefinitely. The samples were embedded using an Automatic Freeze Substitution Unit (AFS) at  $-90^{\circ}\text{C}$  in a solution containing 0.1% tannic acid and 0.5% glutaraldehyde in anhydrous acetone for 24 h and in 2%  $\text{OsO}_4$  in anhydrous acetone for additional 8 h. After a further incubation over 20 h at  $-20^{\circ}\text{C}$  samples were warmed up to  $+4^{\circ}\text{C}$  and washed with anhydrous acetone subsequently. The samples were embedded at room temperature in Agar100 (Epon 812 equivalent) at  $60^{\circ}\text{C}$  over 24h. Images of 70 nm ultrathin sections were taken in a Philips CM120 electron microscope (Philips Inc.) using a TemCam F416 CMOS camera (TVIPS, Gauting, Germany).

## Supplementary Figures

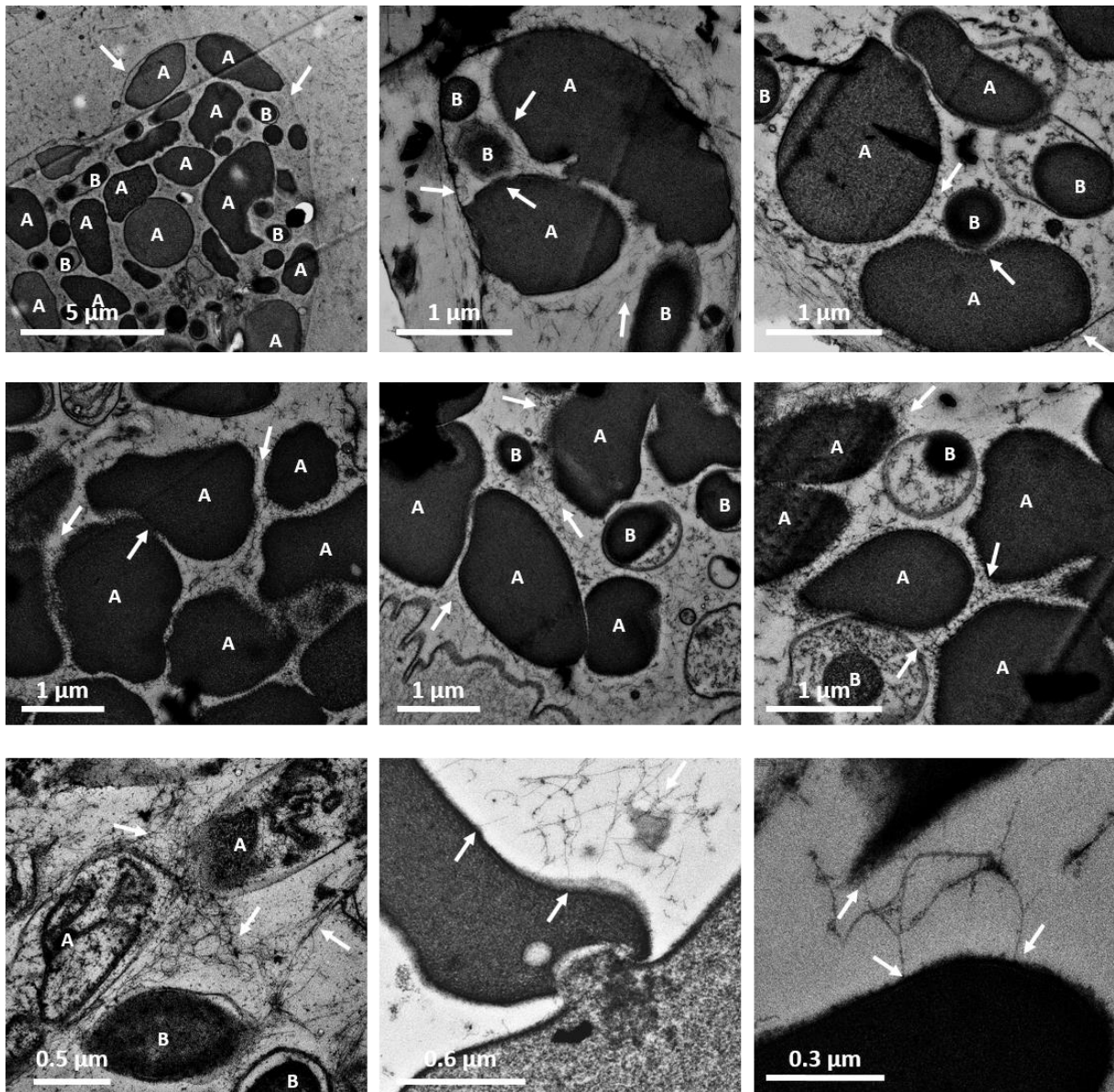


**SI Figure 1. Phylogenetic affiliation of ANME and partner bacteria clades within *Methanomicrobia* and *Deltaproteobacteria*.** In the E20 enrichment ANME-2c forms consortia with Seep-SRB2, in the G37 enrichment ANME-1 forms consortia with Seep-SRB2, and in the G60 enrichment ANME-1 forms consortia with HotSeep-1. The phylogenetic trees are modified from Wegener and colleagues (2016). Phylogeny was inferred with RAxML based on 16S rRNA gene variation; ANME clades are shown in red, partner bacteria clades are shown in green; grey dashed lines connect the dominant partner organisms detected in the consortia. Note that the phylogenetic affiliation of HotSeep-1 based on the 16S rRNA gene is currently not well resolved and its placement within the *Deltaproteobacteria* is debatable (see Dowell *et al.*, 2016; Krukenberg *et al.*, 2016; McKay *et al.*, 2016).

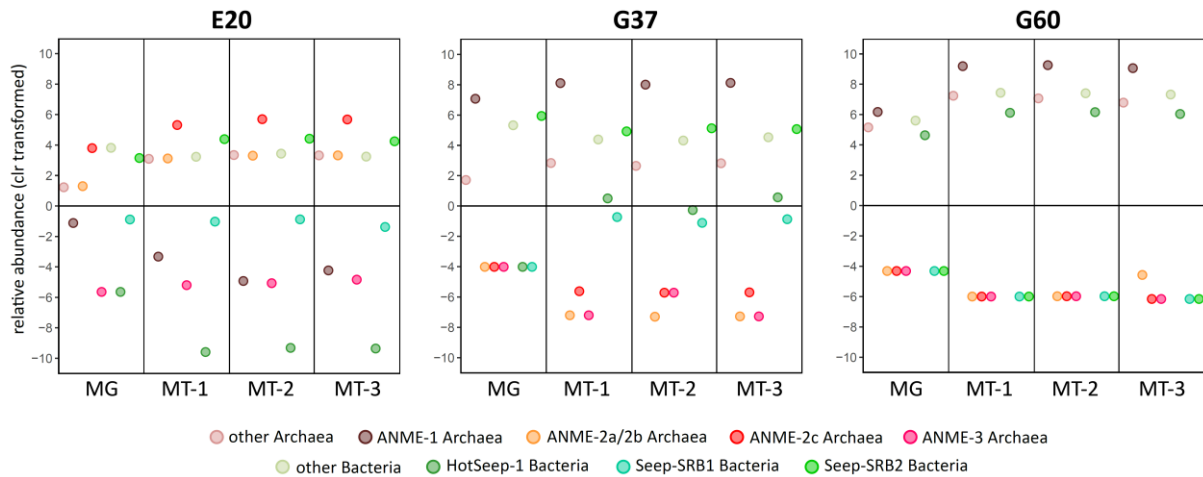


**SI Figure 2. Transmission electron microscopy images of AOM consortia thin sections from the E20 enrichment.** A: Archaeal cells; B: Bacterial cells; arrows point to areas of interest (*i.e.* cell appendages and filaments in the intercellular space).

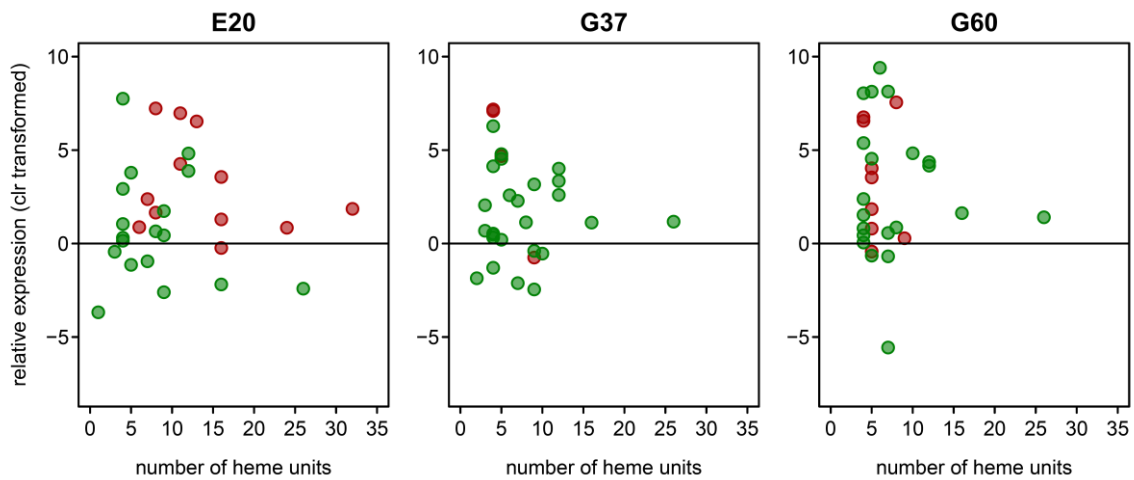




**SI Figure 3. Transmission electron microscopy images of AOM consortia thin sections from the G37 enrichment. A: Archaeal cells; B: Bacterial cells; arrows point to areas of interest (*i.e.* cell appendages and filaments in the intercellular space).**



**SI Figure 4. Relative abundance of 16S rRNA gene and transcript fragments in AOM enrichments E20, G37 and G60.** To account for different sequence counts and compositional effects in the data, the relative abundance of a given clade is shown as a centered log ratio (clr) using a logarithm base of 2. Zero indicates the (geometric) mean abundance level of clades in a given sample, thus positive values indicate greater than the mean abundance while negative values indicate less than the mean abundance. MG: metagenomic; MT: metatranscriptomic (3 replicates).



**SI Figure 5. Relation between heme content and relative expression of c-type cytochromes in ANME and SRB from AOM enrichments E20, G37, G60.** The expression is shown as a centered log ratio (clr) using a logarithm base of 2, relative to the expression of all genes of a specific clade. The line at zero indicates the (geometric) mean expression level, thus positive values indicate greater than mean expression while negative values indicate less than mean expression. Red circles: c-type cytochromes of ANME; green circles: c-type cytochromes of SRB.

## Supplementary Tables

**SI Table 1. Characteristics of the AOM consortia enrichments studied in this work.**

	<b>E20 enrichment</b>	<b>G37 enrichment</b>	<b>G60 enrichment</b>
enrichment temperature	20°C	37°C	50-60°C
source environment	shallow-water seeps off the Island Elba, Italy	deep-sea hydrothermal sediment in Guaymas Basin, Gulf of California, Mexico	deep-sea hydrothermal sediment in Guaymas Basin, Gulf of California, Mexico
<i>in situ</i> temperature	~20°C	~37°C	>50°C
years of <i>in vitro</i> enrichment	4	5	5
enrichment appearance	sediment-free, contains black precipitates	sediment-free, contains black precipitates	sediment-free, contains brownish and crystalline precipitates
dominant consortia members	ANME-2c/ Seep-SRB2	ANME-1a/ Seep-SRB2	ANME-1a/ HotSeep-1
dominant consortia type	mixed type	mixed type	mixed type
typical consortia morphology	aggregates, <100 µm diameter	aggregates, <100 µm diameter	aggregates, >100 µm diameter, brownish-orange color
ANME cell morphology	irregular-shaped cocci sarcina-like packed, ~1 µm cell diameter	irregular-shaped cocci, ~2 µm diameter	rectangular-shaped with cell envelope, ~0.8×1.7 µm
SRB cell morphology	rod-shaped, <0.5×1 µm, often elongated	rod-shaped, 0.5×1 µm	rod-shaped, 0.5×1 µm

**SI Table 2. Classification of metagenomic and metatranscriptomic 16S rRNA gene fragments on different phylogenetic levels.**

See separate excel file with metagenomic (MG) and metatranscriptomic (MT) data for each phylogenetic level (*i.e.* domain, phylum, class, order, family, genus) presented in a separate sheet.

**SI Table 3. Summary of 16S rRNA gene fragments obtained from enrichments E20, G37 and G60 presented as read count data and compositionality corrected data.**

count data	E20				G37				G60			
	MG	MT-1	MT-2	MT-3	MG	MT-1	MT-2	MT-3	MG	MT-1	MT-2	MT-3
other Archaea	58	3300	3245	3290	26	526	493	548	354	4839	4235	3951
ANME-1	11	38	10	17	1086	20299	20215	21610	718	18702	19330	19109
ANME-2a/2b	61	3354	3152	3288	0	0	0	0	0	0	0	1
ANME-2c	347	15366	16594	16874	0	1	1	1	0	0	0	0
ANME-3	0	10	9	11	0	0	1	0	0	0	0	0
other Bacteria	352	3623	3457	3112	323	1543	1571	1798	484	5544	5351	5726
HotSeep-1	0	0	0	0	0	104	65	115	247	2218	2256	2352
Seep-SRB1	13	189	173	126	0	44	36	42	0	0	0	0
Seep-SRB2	221	8081	6827	6242	494	2237	2750	2614	0	0	0	0
clr transformed data	E20				G37				G60			
	MG	MT-1	MT-2	MT-3	MG	MT-1	MT-2	MT-3	MG	MT-1	MT-2	MT-3
other Archaea	1.2	3.1	3.3	3.3	1.7	2.8	2.6	2.8	5.2	7.2	7.1	6.8
ANME-1	-1.1	-3.3	-4.9	-4.2	7.1	8.1	8.0	8.1	6.2	9.2	9.3	9.1
ANME-2a/2b	1.3	3.1	3.3	3.3	-4.0	-7.2	-7.3	-7.3	-4.3	-6.0	-6.0	-4.6
ANME-2c	3.8	5.3	5.7	5.7	-4.0	-5.6	-5.7	-5.7	-4.3	-6.0	-6.0	-6.2
ANME-3	-5.6	-5.2	-5.1	-4.8	-4.0	-7.2	-5.7	-7.3	-4.3	-6.0	-6.0	-6.2
other Bacteria	3.8	3.2	3.4	3.2	5.3	4.4	4.3	4.5	5.6	7.4	7.4	7.3
HotSeep-1	-5.6	-9.6	-9.3	-9.4	-4.0	0.5	-0.3	0.6	4.6	6.1	6.2	6.0
Seep-SRB1	-0.9	-1.0	-0.9	-1.4	-4.0	-0.7	-1.1	-0.9	-4.3	-6.0	-6.0	-6.2
Seep-SRB2	3.1	4.4	4.4	4.2	5.9	4.9	5.1	5.1	-4.3	-6.0	-6.0	-6.2

**SI Table 4. Comparison of 16S rRNA and metabolic marker genes of ANME and SRB.** Sequence identity (id) and coverage (cov) are determined by pairwise alignment using blastn (Zhang *et al.*, 2000) or blastp (Altschul *et al.*, 2005).

<b>16S rRNA gene nucleotide sequence (accession number)</b>				
	ANME-2c_E20 (C4B59_07810)	ANME-1a_G37 (C4B55_01375)	ANME-1a_G60 (C4B56_03475)	ANME-1b (FP565147.1)
ANME-2c_E20 (C4B59_07810)	-	81% id/66% cov	84% id/92% cov	82% id/98% cov
ANME-1a_G37 (C4B55_01375)	81% id/84% cov	-	91% id/94% cov	89% id/98% cov
ANME-1a_G60 (C4B56_03475)	84% id/96% cov	91% id/78% cov	-	92% id/99% cov
ANME-1b (FP565147.1)	82% id/99% cov	89% id/80% cov	92% id/97% cov	-
<b>McrA amino acid sequence (accession number)</b>				
	ANME-2c_E20 (C4B59_08440)	ANME-1a_G37 (C4B55_02545)	ANME-1a_G60 (C4B56_08905)	ANME-1b (CBH39484.1)
ANME-2c_E20 (C4B59_08440)	-	49% id/97% cov	50% id/97% cov	48% id/96% cov
ANME-1a_G37 (C4B55_02545)	49% id/97% cov	-	88% id/100% cov	89% id/98% cov
ANME-1a_G60 (C4B56_08905)	50% id/97% cov	88% id/100% cov	-	84% id/98% cov
ANME-1b (CBH39484.1)	48% id/97% cov	89% id/100% cov	84% id/100% cov	-
<b>16S rRNA gene nucleotide sequence (accession number)</b>				
	Seep-SRB2_E20 (C4B58_05045)	Seep-SRB2_G37 (C4B57_05185)	HotSeep-1 (HS1_RS01390)	
Seep-SRB2_E20 (C4B58_05045)	-	97% id/99% cov	85% id/99% cov	
Seep-SRB2_G37 (C4B57_05185)	97% id/99% cov	-	85% id/99% cov	
HotSeep-1_G60 (HS1_RS01390)	85% id/99% cov	85% id/100% cov	-	
<b>DsrA amino acid sequence (accession number)</b>				
	Seep-SRB2_E20 (C4B58_02260)	Seep-SRB2_G37 (C4B57_06465)	HotSeep-1 (HS1_RS10950)	
Seep-SRB2_E20 (C4B58_02260)	-	88% id/100% cov	67% id/90% cov	
Seep-SRB2_G37 (C4B57_06465)	88% id/100% cov	-	72% id/90% cov	
HotSeep-1 (HS1_RS10950)	67% id/98% cov	72% id/98% cov	-	

**SI Table 5. Single copy genes identified in ANME draft genomes.** Single copy genes were identified with CheckM (Parks *et al.*, 2015).

See separate excel file with archaeal and euryarchaeal single copy gene data in separate sheets.

**SI Table 6. Overview of gene expression data of ANME and SRB.** Included are genes central to this study with manually refined annotations and expression data from three transcriptomic replicates.

See separate excel file with separate sheets for data from ANME and SRB.

**SI Table 7. Draft genomes and expression data generated in this study.** The gene descriptions are automatic annotations derived from NCBI's Prokaryotic Genome Annotation Pipeline (for manually curated annotations of genes relevant to this study see SI Table 6). For each gene the expression data from three transcriptomic replicates are included as raw counts and as centered log ratio transformed values.

See separate excel file with data for each ANME and SRB studied presented in a separate sheet.

**SI Table 8. Overview of c-type cytochromes encoded in the ANME and SRB draft genomes.** Included are expression data (as count values and centered log (log<sub>2</sub>) ratio transformed values), number of detected CXXCH motifs indicative of heme-binding sites, cytochrome C class according to best scoring protein domain model in the pfamA or TIGRFAM databases and subcellular localization prediction based on psortb analysis.

See separate excel file with data for each of the analyzed ANME and SRB presented in a separate sheet.

**SI Table 9. Overview of clade specific oligonucleotide probes used in CARD-FISH experiments in this study.**

Probe	Specificity (target group)	Oligonucleotide sequence (5'-3')	Target site <sup>1</sup>	FA (%) <sup>2</sup>	Reference
ANME1-350	ANME-1 archaea	AGTTTTCGCGCCTGATGC	350-367	40	Boetius <i>et al.</i> , 2000
ANME-2-538	ANME-2 archaea	GGCTACCACTCGGGCCGC	538-555	50	Treude <i>et al.</i> , 2005
HotSeep-1-1456	HotSeep-1 cluster	CGCCGACCACACCTTGGG	183-201	30	Krukenberg <i>et al.</i> , 2016
SEEP2-658	SEEP-SRB2 cluster	TCCA <sup>c</sup> CTCCCTCTCCGGT	658-685	45	Kleindienst <i>et al.</i> , 2012
cSEEP2-658 <sup>3</sup>	<i>Desulfosarcina/Desulfococcus</i> cluster	TCCA <sup>c</sup> CTCCCTCTCC <u>CA</u> T	658-685	-	Kleindienst <i>et al.</i> , 2012

<sup>1</sup>Nucleotide position in the 16S RNA gene of *Escherichia coli*.

<sup>2</sup>Formamide (FA) concentration used in the hybridization buffer.

<sup>3</sup>Used as unlabeled competitor (c) oligonucleotide in hybridizations with probe SEEP2-658; underlined bases are different to SEEP2-658. This probe corresponds to an unlabeled version of probe DSS-658 targeting members of the *Desulfosarcina/Desulfococcus* cluster.

## References

- Altschul SF, Wootton JC, Gertz EM, Agarwala R, Morgulis A, Schäffer AA, *et al.* (2005). Protein database searches using compositionally adjusted substitution matrices. *FEBS J* **272**: 5101–5109.
- Bankevich A, Nurk S, Antipov D, Gurevich AA, Dvorkin M, Kulikov AS, *et al.* (2012). SPAdes: A new genome assembly algorithm and its applications to single-cell sequencing. *J Comput Biol* **19**: 455–477.
- Boetius A, Ravensschlag K, Schubert CJ, Rickert D, Widdel F, Gieseke A, *et al.* (2000). A marine microbial consortium apparently mediating anaerobic oxidation of methane. *Nature* **407**: 623–626.
- Dowell F, Cardman Z, Dasarathy S, Kellermann MY, Lipp JS, Ruff SE, *et al.* (2016). Microbial communities in methane- and short chain alkane-rich hydrothermal sediments of the Guaymas Basin. *Front Microbiol* **7**: 17.
- Gurevich A, Saveliev V, Vyahhi N, Tesler G. (2013). QUAST: quality assessment tool for genome assemblies. *Bioinformatics* **29**: 1072–1075.
- Holler T, Widdel F, Knittel K, Amann R, Kellermann MY, Hinrichs K-U, *et al.* (2011). Thermophilic anaerobic oxidation of methane by marine microbial consortia. *ISME J* **5**: 1946–56.
- Kleindienst S, Ramette A, Amann R, Knittel K. (2012). Distribution and *in situ* abundance of sulfate-reducing bacteria in diverse marine hydrocarbon seep sediments. *Environ Microbiol* **14**: 2689–2710.
- Krukenberg V, Harding K, Richter M, Glöckner FO, Gruber-Vodicka HR, Adam B, *et al.* (2016). *Candidatus* Desulfosphaerulum auxilii, a hydrogenotrophic sulfate-reducing bacterium involved in the thermophilic anaerobic oxidation of methane. *Environ Microbiol* **18**: 3073–3091.
- McGlynn SE, Chadwick GL, Kempes CP, Orphan VJ. (2015). Single cell activity reveals direct electron transfer in methanotrophic consortia. *Nature* **526**: 531–535.
- McKay L, Klokman VW, Mendlovitz HP, LaRowe DE, Hoer DR, Albert D, *et al.* (2015). Thermal and geochemical influences on microbial biogeography in the hydrothermal sediments of Guaymas Basin, Gulf of California. *Environ Microbiol Rep* **8**: 150–161.
- Parks DH, Imelfort M, Skennerton CT, Hugenholtz P, Tyson GW, Centre A, *et al.* (2015). CheckM: assessing the quality of microbial genomes recovered from isolates, single cells, and metagenomes. *Genome Res* **7**: 1043–1055.
- Pernthaler A, Amann R. (2004). Simultaneous fluorescence *in situ* hybridization of mRNA and rRNA in environmental bacteria. *Appl Environ Microbiol* **70**: 5426–5433.
- Ruff SE, Kuhfuss H, Wegener G, Lott C, Ramette A, Wiedling J, *et al.* (2016). Methane seep in shallow-water permeable sediment harbors high diversity of anaerobic methanotrophic communities, Elba, Italy. *Front Microbiol* **7**: 374.
- Strous M, Kraft B, Bisdorf R, Tegetmeyer HE. (2012). The binning of metagenomic contigs for microbial physiology of mixed cultures. *Front Microbiol* **3**: 410.
- Treude T, Krüger M, Boetius A, Jørgensen BB. (2005). Environmental control on anaerobic oxidation of methane in the gassy sediments of Eckernförde Bay (German Baltic). *Limnol Oceanogr* **50**: 1771–1786.
- Wegener G, Krukenberg V, Ruff SE, Kellermann MY, Knittel K. (2016). Metabolic

capabilities of microorganisms involved in and associated with the anaerobic oxidation of methane. *Front Microbiol* **7**: 46.

Widdel F, Bak F. (1992). Gram negative mesophilic sulphate-reducing bacteria. In *The Prokaryotes*. Balows A, Trüper HG, Dworkin M, Harder W, and Schleifer K-H (eds). New York, USA. *Springer*, pp. 3352–3378.

Zhang Z, Schwartz S, Wagner L, Miller W. (2000). A greedy algorithm for aligning DNA sequences. *J Comput Biol* **7**: 203–14.

Zhou J, Bruns MANN, Tiedje JM. (1996). DNA recovery from soils of diverse composition. *Appl Environ Microbiol* **62**: 316–322.